On the Dynamics of a Nonlinear Continuous Random System

Americo Barbosa da Cunha Junior
Rubens Sampaio

Department of Mechanical Engineering
Pontifícia Universidade Católica do Rio de Janeiro
{americo,rsampaio}@puc-rio.br

1st International Symposium on
Uncertainty Quantification and Stochastic Modeling
February 26th to March 2nd, 2012
Maresias - SP - Brazil

Outline

PUC RIO

Work Context and Objectives

This work is a first effort to study the dynamics of a nonlinear one-dimensional elastic bar, subject to uncertainties in the system parameters (external forcing, boundary and initial conditions, etc) using Monte Carlo simulations, in a cloud computing framework, to compute uncertainty propagation.

The main objectives of this work are:

- Discuss in details the deterministic modeling of the bar;
- Construct a stochastic model for the bar using probability theory and maximum entropy principle;
- Use Monte Carlo simulations to characterize the dynamical behavior of the random system.

Physical Model

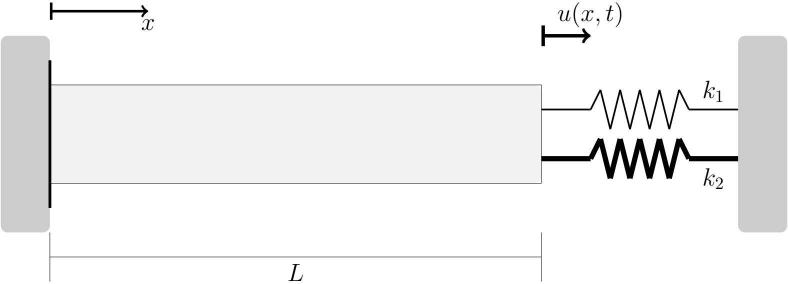

Figure: Sketch of a bar fixed at one end attached to two springs on the other extreme.

Strong Formulation

Find a displacement field $u : [0, L] \times [0, +\infty) \to \mathbb{R}$ that satisfies

$$\rho A \frac{\partial^2 u}{\partial t^2}(x, t) = \frac{\partial}{\partial x}\left(EA \frac{\partial u}{\partial x}(x, t) \right) + f(x, t),$$

for all $(x, t) \in (0, L) \times (0, +\infty)$, as well as the boundary conditions

$$u(0, t) = 0 \quad \text{and} \quad EA \frac{\partial u}{\partial x}(L, t) = -k_1 u(L, t) - k_2 \left[u(L, t) \right]^3,$$

for all $t \in [0, +\infty)$, and the initial conditions

$$u(x, 0) = u_0(x) \quad \text{and} \quad \frac{\partial u}{\partial t}(x, 0) = v_0(x),$$

for all $x \in [0, L]$.

Variational Formulation (1/2)

Find a displacement field $u : [0, L] \times [0, +\infty) \to \mathbb{R}$ that satisfies

$$\mathcal{M}(u, w) + \mathcal{K}(u, w) = \mathcal{F}(w) + \mathcal{G}(u, w),$$

for all w in

$$W = \left\{ w : [0, L] \to \mathbb{R} \;\; \middle| \;\; \int_0^L \big[w(x) \big]^2 \, dx < +\,\infty \;\; \text{and} \;\; w(0) = 0 \right\},$$

as well as the weak form of initial displacement

$$\int_0^L \rho A u(x, 0) w(x) dx = \int_0^L \rho A u_0(x) w(x) dx,$$

and the weak form of initial velocity

$$\int_0^L \rho A \frac{\partial u}{\partial t}(x, 0) w(x) dx = \int_0^L \rho A v_0(x) w(x) dx.$$

Variational Formulation (2/2)

- $\mathcal{M}$ is the mass operator

$$\mathcal{M}(u, w) = \int_0^L \rho A \, \frac{\partial^2 u}{\partial t^2}(x, t) w(x) dx$$

- $\mathcal{K}$ is the stiffness operator

$$\mathcal{K}(u, w) = \int_0^L EA \, \frac{\partial u}{\partial x}(x, t) \, \frac{\partial w}{\partial x}(x) dx + k_1 u(L, t) w(L)$$

- $\mathcal{F}$ is the external force operator

$$\mathcal{F}(w) = \int_0^L f(x, t) w(x) dx$$

- $\mathcal{G}$ is the nonlinear force operator

$$\mathcal{G}(u, w) = -k_2 \left[u(L, t) \right]^3 w(L)$$

An Eigenvalue Problem (1/2)

Initially, consider the homogeneous equation that is associated to the variational formulation,

$$\mathcal{M}(u, w) + \mathcal{K}(u, w) = 0.$$

Now assume that the above equation has a solution of the form $u(x,t) = e^{i\nu t}\phi(x)$, where ν is the natural frequency, ϕ is shape mode and i is the imaginary unit $(\sqrt{-1})$.

PUC RIO

An Eigenvalue Problem (2/2)

Replacing the expression of u and using the linearity of the operators $\mathcal{M}$ and $\mathcal{K}$, one gets

$$\left[-\nu^2 \mathcal{M}(\phi, w) + \mathcal{K}(\phi, w)\right] e^{i\nu t} = 0.$$

Since $e^{i\nu t} \neq 0$ for all t, the last equation is equivalent to

$$-\nu^2 \mathcal{M}(\phi, w) + \mathcal{K}(\phi, w) = 0,$$

a generalized eigenvalue problem with denumerable number of solutions (ν_n^2, ϕ_n). The eigenfunctions $\{\phi_n\}_{n=1}^{+\infty}$ span the space of functions which contains the solution of the variational equation.

Orthogonal Shape Modes (1/3)

It is possible to show that a pair of solutions for the generalized eigenvalue problem above, (ν_n^2, ϕ_n) and (ν_m^2, ϕ_m), with $\nu_m \neq \nu_n$, satisfy the following relations of orthogonality

$$\mathcal{M}(\phi_n, \phi_m) = 0,$$

and

$$\mathcal{K}(\phi_n, \phi_m) = 0.$$

They are good choices for basis function when one uses a weighted residual procedure to approximate the nonlinear variational equation solution.

Orthogonal Shape Modes (2/3)

The bar, fixed at one end, and attached to a linear spring on the other (fixed-spring bar), has natural frequencies and orthogonal shape modes given by

$$\nu_n = \lambda_n \frac{c}{L} \qquad \text{and} \qquad \phi_n(x) = \sin\left(\lambda_n \frac{x}{L}\right),$$

where $c = \sqrt{E/\rho}$ and the λ_n are the solutions of

$$\cot\left(\lambda_n\right) + \left(\frac{k_1 L}{AE}\right)\frac{1}{\lambda_n} = 0,$$

for $n = 1, \cdots, \infty$.

Orthogonal Shape Modes (3/3)

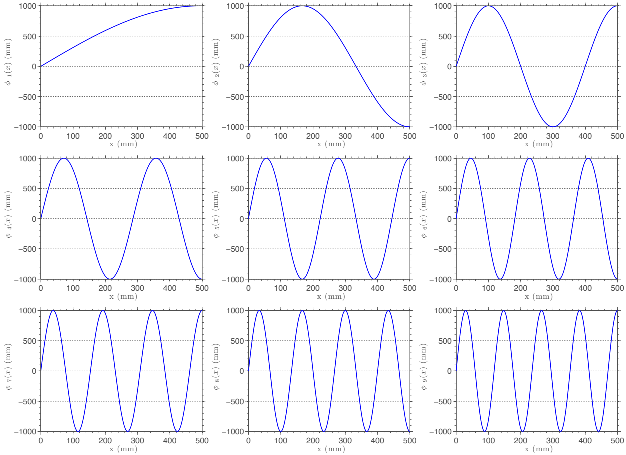

Figure: Sketch of first nine orthogonal shape modes of a fixed-spring bar.

Model Equation Discretization

The Galerkin method is used to approximate the solution of the variational equation

$$u^N(x,t) = \sum_{n=1}^{N} U_n(t)\phi_n(x),$$

where ϕ_n are the orthogonal shape modes and the coefficients U_n are time-dependent functions. This procedure results in a $N \times N$ set of nonlinear ordinary differential equations

$$[M]\,\ddot{\mathbf{U}}(t) + [K]\,\mathbf{U}(t) = \mathbf{F}(t) - \mathbf{G}\left(\mathbf{U}(t)\right),$$

supplemented by a pair of initial conditions

$$\mathbf{U}(0) = \mathbf{U}_0 \quad \text{and} \quad \dot{\mathbf{U}}(0) = \mathbf{V}_0.$$

Nonlinear ODE System Solution (1/2)

An approximation for the solution of the initial value problem (IVP) above is computed by Newmark method, which defines the following integration scheme

$$\mathbf{v}_{n+1} = \mathbf{v}_n + (1-\gamma)\Delta t \mathbf{a}_n + \gamma \Delta t \mathbf{a}_{n+1},$$

$$\mathbf{d}_{n+1} = \mathbf{d}_n + \Delta t \mathbf{v}_n + \left(\frac{1}{2} - \beta\right) \Delta t^2 \mathbf{a}_n + \beta \Delta t^2 \mathbf{a}_{n+1}.$$

where $\mathbf{d}_n$, $\mathbf{v}_n$ and $\mathbf{a}_n$ are approximations to $\mathbf{U}(t_n)$, $\dot{\mathbf{U}}(t_n)$ and $\ddot{\mathbf{U}}(t_n)$, respectively. The Newmark scheme replaced in the IVP defines a nonlinear system of algebraic equations with unknowns $\mathbf{d}_n$, $\mathbf{v}_n$ and $\mathbf{a}_n$.

Nonlinear ODE System Solution (2/2)

This nonlinear system of algebraic equations has an approximation for its solution constructed by Newton-Rapson method

$$\mathbf{a}_{n+1}^{(k+1)} = \mathbf{a}_{n+1}^{(k)} + \frac{1}{\beta \Delta t^2} \Delta \mathbf{d},$$

$$\mathbf{v}_{n+1}^{(k+1)} = \mathbf{v}_{n+1}^{(k)} + \frac{\gamma}{\beta \Delta t} \Delta \mathbf{d},$$

$$\mathbf{d}_{n+1}^{(k+1)} = \mathbf{d}_{n+1}^{(k)} + \Delta \mathbf{d},$$

where $\Delta \mathbf{d}$ is the solution of

$$\left(\frac{1}{\beta \Delta t^2} \frac{\partial \mathbf{r}}{\partial \mathbf{a}} + \frac{\gamma}{\beta \Delta t} \frac{\partial \mathbf{r}}{\partial \mathbf{v}} + \frac{\partial \mathbf{r}}{\partial \mathbf{d}} \right) \Delta \mathbf{d} = -\mathbf{r} \left(\mathbf{a}^*, \mathbf{v}^*, \mathbf{d}^* \right),$$

being the residual vector $\mathbf{r}$ defined by

$$\mathbf{r} \left(\mathbf{a}, \mathbf{v}, \mathbf{d} \right) = [M] \, \mathbf{a} + [K] \, \mathbf{d} - \left(\mathbf{F}(t) - \mathbf{G} \left(\mathbf{d} \right) \right).$$

Probabilistic Model

Consider a probability space $(\Omega, \mathbb{A}, \mathbb{P})$ and assume that the elastic modulus is a random variable $E : \Omega \to (0, \infty)$.

Now the displacement of the bar is a random field

$$U : \Omega \times [0, L] \times [0, +\infty) \to \mathbb{R},$$

which satisfies the following stochastic partial differential equation

$$\rho A \frac{\partial^2 U}{\partial t^2}(\omega, x, t) = \frac{\partial}{\partial x}\left(E(\omega) A \frac{\partial U}{\partial x}(\omega, x, t) \right) + f(x, t),$$

being the partial derivatives now defined in the mean square sense.

This problem has boundary and initial conditions similar to those defined in deterministic case, by changing u for U only.

Elastic Modulus Distribution

The maximum entropy principle is used to obtain the probability distribution of the elastic modulus subjected to the constraints:

- the support of E is the interval $(0, +\infty)$;
- the mean value of E is specified;
- the displacement of the bar has finite variance.

In this case, the probability density function with maximum entropy is that one which corresponds to the gamma distribution.

So it is assumed that the random variable E is gamma distributed, with mean $\mu_E = 203\ GPa$ and dispersion factor $\delta_E = 0.1$.

Stochastic Solver

The uncertainty propagation of the stochastic model that describes the bar dynamics is computed by Monte Carlo method:

- An ensemble of 4^5 realizations is used to sample the random space Ω;
- The realizations of $E : \Omega \to (0, \infty)$ are generated by Matlab pseudorandom number generator (Mersenne twister).

Informations about the random bar are obtained from:

- Statistics of the random field U, such as the mean value and variance;
- Histograms of U, for fixed values of x and t.

Case 1: Linear Spring

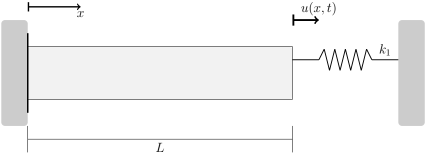

- $\rho = 7900 \ kg/m^3$
- $L \ = \ 500 \ mm$
- $A = 625\pi \ mm^2$
- $k_1 = 1.3 \times 10^6 \ N/m$
- $k_2 = 0 \ N/m^3$
- $\alpha = 0.1 \ mm$
- $\sigma = 100 \ kN/m$
- $f(x,t) = \sigma \sin\left(\lambda_1 \frac{x}{L}\right) \sin(\nu_1 t)$
- $u_0(x) = \alpha \sin\left(\lambda_3 \frac{x}{L}\right) + \frac{x}{2000}$
- $v_0(x) = 0$

Case 2: Linear and Nonlinear Springs

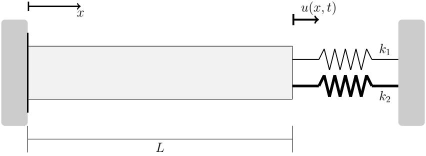

- $\rho = 7900 \ kg/m^3$
- $L \ = \ 500 \ mm$
- $A = 625\pi \ mm^2$
- $k_1 = 1.3 \times 10^6 \ N/m$
- $k_2 = 5.0 \times 10^{15} \ N/m^3$
- $\alpha = 0.1 \ mm$
- $\sigma = 100 \ kN/m$
- $f(x,t) = \sigma \sin\left(\lambda_1 \frac{x}{L}\right) \sin(\nu_1 t)$
- $u_0(x) = \alpha \sin\left(\lambda_3 \frac{x}{L}\right) + \frac{x}{2000}$
- $v_0(x) = 0$

Convergence of Shape Modes for Case 1

N	$\lVert\cdot\rVert_{L_2}$	$\lVert\cdot\rVert_{H^1}$
5	$\sim 8.1 \times 10^{-5}$	$\sim 3.7 \times 10^{-4}$
10	$\sim 9.9 \times 10^{-7}$	$\sim 3.9 \times 10^{-5}$
15	$\sim 2.9 \times 10^{-7}$	$\sim 2.2 \times 10^{-5}$
20	$\sim 1.3 \times 10^{-7}$	$\sim 1.4 \times 10^{-5}$
25	$\sim 7.7 \times 10^{-8}$	$\sim 1.1 \times 10^{-5}$
30	$\sim 5.7 \times 10^{-8}$	$\sim 9.6 \times 10^{-6}$

An approximation with 10 modes incurs an error of $\mathcal{O}(10^{-6})$ in L_2 norm and an error of $\mathcal{O}(10^{-4})$ considering H^1 norm.

Convergence of Shape Modes for Case 2

N	$\|\cdot\|_{L_2}$	$\|\cdot\|_{H^1}$
5	$\sim 1.4 \times 10^{-4}$	$\sim 6.0 \times 10^{-4}$
10	$\sim 2.3 \times 10^{-6}$	$\sim 6.7 \times 10^{-5}$
15	$\sim 5.1 \times 10^{-7}$	$\sim 2.4 \times 10^{-5}$
20	$\sim 2.4 \times 10^{-7}$	$\sim 1.6 \times 10^{-5}$
25	$\sim 1.5 \times 10^{-7}$	$\sim 1.2 \times 10^{-5}$
30	$\sim 1.0 \times 10^{-7}$	$\sim 1.1 \times 10^{-5}$

An approximation with 10 modes incurs an error of $\mathcal{O}(10^{-6})$ in L_2 norm and an error of $\mathcal{O}(10^{-4})$ considering H^1 norm.

Envelope of Reliability for $U(L,\cdot)$

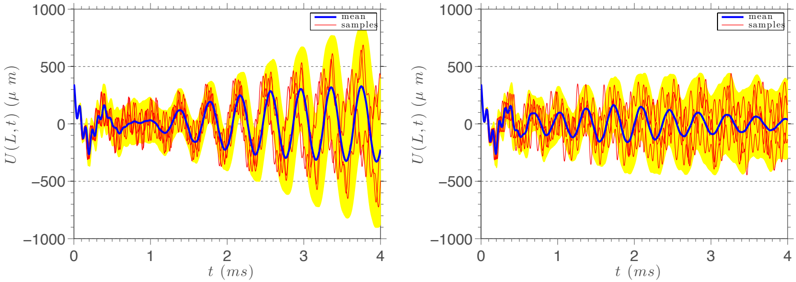

(a) case 1 (b) case 2

Figure: This figure illustrates the mean value, some realizations and the interval of confidence (with two standard deviations) for the random process $U(L,\cdot)$

Mean Value of $U(L, \cdot)$

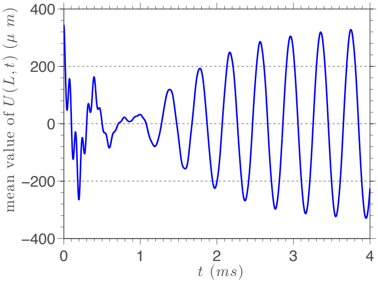

(a) case 1

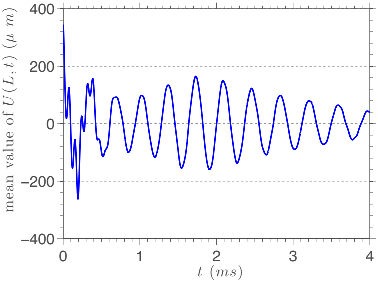

(b) case 2

Figure: This figure illustrates in detail the mean value of $U(L, \cdot)$.

Spectral Density Function of $U(L,\cdot)$

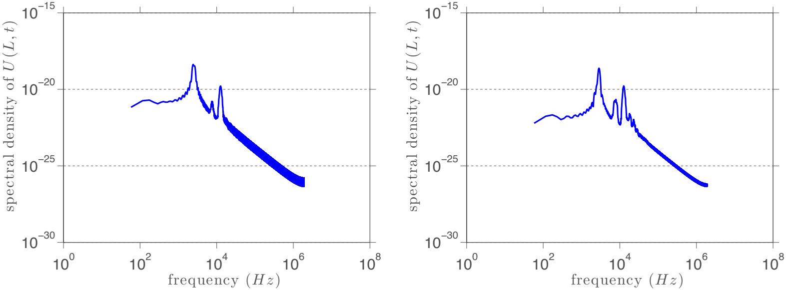

(a) case 1 (b) case 2

Figure: This figure illustrates the spectral density function of $U(L,\cdot)$.

Envelope of Reliability for $U(\cdot, T)$

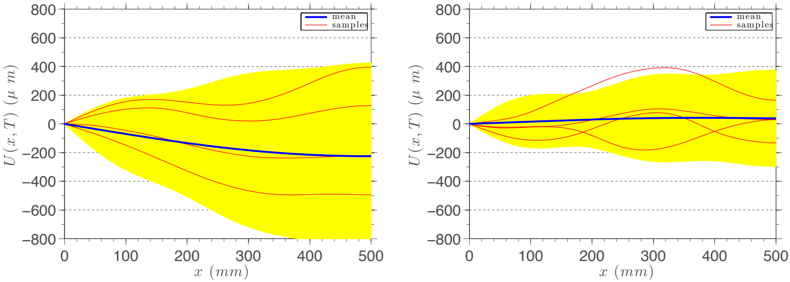

(a) Case 1 (b) Case 2

Figure: This figure illustrates the mean value, some realizations and the interval of confidence (with two standard deviations) for the random field $U(\cdot, T)$ where $T = 4$ ms.

Mean Value of $U(\cdot, T)$

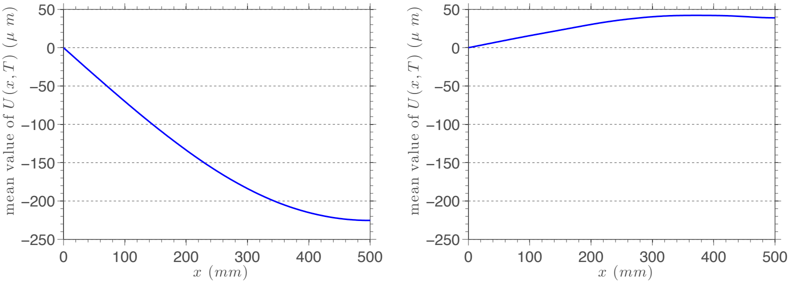

(a) Case 1 (b) Case 2

Figure: This figure illustrates in detail the mean value of $U(\cdot, T)$ where $T = 4\ ms$.

Histogram of $U(L,T)$

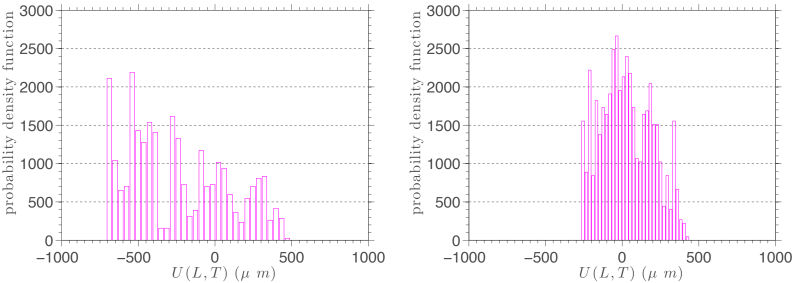

(a) Case 1

(b) Case 2

Figure: Comparison between the PDFs of U for $x = L$ and $t = T = 4\ ms$.

Final Remarks

- There are similarities and differences in the behavior of the two systems analyzed;
- For the analyzed parameters values, the nature of the spring has little interference in the spatial behavior of the bar right extreme, but the nonlinearity affects significantly its temporal behavior;
- Further analysis are necessary to better understand the nonlinear dynamics of this bar.

Work in Progress

- Study of the nonlinearity effect in uncertainty propagation of a random bar with variable cross-sectional area;
- Development of a cloud computing framework, McCloud, to efficiently run Monte Carlo (MC) simulations;
- It is expected to run MC simulations with a few hundred of thousands of realizations in order to decrease statistical bias of calculations.

Acknowledgments

Discussions and suggestions:

- Prof. Mario Escalante — Universidad Tecnológica Nacional
- Prof. Olivier Le Maître — CNRS
- Prof. Thiago Ritto — UFRJ
- Dr. Julien Mauprivez — PUC–Rio

Partnership in McCloud project:

- Prof. Helio Lopes — PUC–Rio
- Prof. Karin Breitman — PUC–Rio
- Eng. Rafael Nasser — PUC–Rio

Financial support:

- CNPq
- FAPERJ

References

- H. Brezis, **Functional Analysis, Sobolev Spaces and Partial Differential Equations**. New York: Springer, 2010.
- T. J. R. Hughes, **The Finite Element Method**. New York: Dover Publications, 2000.
- R. W. Shonkwiler and F. Mendivil, **Explorations in Monte Carlo Methods**. New York: Springer, 2009.
- C. Soize, A nonparametric model of random uncertainties for reduced matrix models in structural dynamics. **Probabilistic Engineering Mechanics**, Vol. 15 pp. 277 – 294, 2000.
- R. Nasser; K. Breitman; H. Lopes; **McCloud: Monte Carlo Service in Windows Azure**. in preparation.